Study on Vibration Characteristics of IPMSM According to Number of Poles/Slots and Winding Method

Mun-Seok Jang[1], Jae-Seung Lee[1], Si-Uk Jung[1], Dae-kyu Jang[2] and Jae-Woo Jung[1], *Member*, *IEEE*

[1]Department of Electrical Engineering, Daegu University, Gyeongsan 38453, Republic of Korea,
wkd5410@daegu.ac.kr, qsd1645@daegu.ac.kr, jsu9085@daegu.ac.kr, jjw@daegu.ac.kr
[2]Department of Motor Advanced R&D Team, LG Electronics, Changwon 51554, Republic of Korea
daekyu.jang@lge.com

The interior permanent magnet synchronous motor (IPMSM) is widely used in various industrial products due to its high torque density and efficiency. Vibration and noise generated from the motor can cause user discomfort and shortened life of the product. After designing the distributed winding model with full-pitch and short-pitch winding methods and the concentrated winding model, the excitation force generated on one tooth was evaluated through two-dimensional(2-D) finite element analysis (FEA). In addition, the space-time harmonic analysis of the air-gap flux density was performed to derive the spectrum of the air gap flux density and pressure. Finally, the electromagnetic characteristics derived through the 2-D FEA were mapped to the three-dimentional mechanical frequency analysis to comprehensively evaluate the displacement and acceleration outside the stator.

***Index Terms*—AC Machines, Harmonic analysis, Permanent magnet motors, Vibrations**

I. Introduction

The interior permanent magnet synchronous motor (IPMSM) has been widely adopted in a variety of industrial applications, including home appliances, defense systems, and electric vehicles, owing to its high torque density and superior efficiency [1]. Among these applications, the IPMSMs used in home appliances are spatially located near users, making the vibration and noise generated by the motor critical factors influencing consumer purchasing decisions. In addition, excessive vibration generated by the IPMSM is one of the primary causes of reduced product lifespan. Therefore, various studies have been conducted on the design and control methods of IPMSMs aimed at reducing vibration and noise. fractional-slot concentrated winding (FSCW) is currently favored due to its lower manufacturing cost and higher efficiency, attributed to shorter end-turns [2]. Since concentrated windings generate a significant amount of harmonic components, they result in greater core losses compared to distributed windings and exhibit inferior vibration and noise characteristics. With advancements in manufacturing and material technologies, distributed windings are expected to be reintroduced in home appliance motors in the near future. In this study, the vibration characteristics of IPMSMs for home appliances were investigated with respect to various pole/slot combinations and winding methods. In terms of the design approach, a simplified design methodology was employed to generalize the motor, and an identical procedure was applied for each combination of pole and slot numbers. Subsequently, the pulse width modulation (PWM) current obtained through dynamic simulations in MATLAB Simulink was applied to each model to reflect the electrical and vibration characteristics induced by the PWM excitation. For the comparative analysis, models with a slots per pole per phase q of 0.5 and 2 were considered. The q=0.5 model employed a concentrated winding configuration, whereas the q=2 model was designed with a distributed winding.

II. Design for Each Model

In this study, 6-pole and 8-pole models were adopted as design specifications for 3-phase windings. The model with q=2 was designed as a full-pitch model with an overlap angle pole, β of 6/6 slot pitch and a short-pitch model with β of 5/6 slot pitch. The motor shapes for each model are as shown in Fig. 1. In this two-page paper, only the results of the 6-pole, 9-slot model are presented due to space constraints. The design methodology based on the number of poles and slots is outlined as follows. The number of series turns per phase, the width of the permanent magnet, and the yoke thickness were inversely proportional to the number of poles, and the tooth width and slot opening length were inversely proportional to the number of slots to design the IPMSM. In order to obtain a similar no-load back electromotive force (EMF) to secure the target output for each model, the stack length was adjusted, no-load back EMF of the 6-pole, 9-slot model is 30.14 V_{rms}, the stack length is 40 mm, and the series resistance is 2.081 Ω.

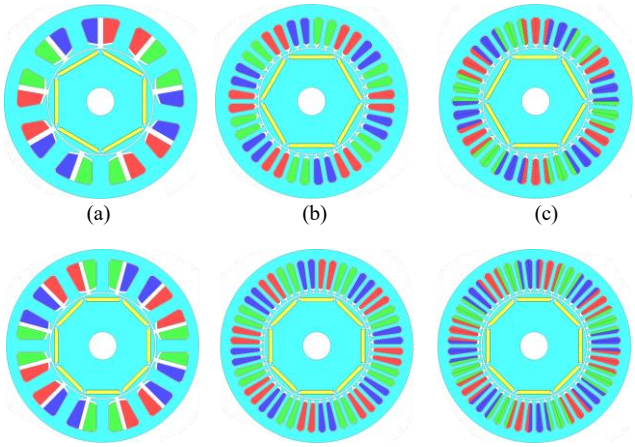


Fig. 1. Shape for each model. (a) 6-pole, 9-slot model. (b) 6-pole, 36-slot full-pitch model. (c) 6-pole, 36-slot short-pitch model. (d) 8-pole, 12-slot model. (e) 8-pole, 48-slot full-pitch model. (f) 8-pole, 48-slot short-pitch model.

III. Vibration Characteristics for 6-Pole, 9-Slot Model

To analyze the vibration characteristics, the following analyses were conducted: excitation force acting on a single stator tooth, radial magnetic flux density, displacement of stator, and acceleration response. For each model, d-axis and q-axis equivalent circuit analyses were performed to evaluate the characteristics across the entire operating range and to derive the motor performance. Based on the motor performance, the PWM current was derived and subsequently applied through dynamic simulation under a switching frequency of 4000 Hz, with a load condition of 1560 rpm and 1.54 Nm. Fig. 2 shows the excitation force generated on a single stator tooth in the 6-pole, 9-slot model under load operation. For the 6-pole, 9-slot model, the peak-to-peak value of the excitation force value is 113.40 N, and the average force value is 116.33 N. When analyzing the vibration and noise characteristics based on the excitation force acting on the stator teeth, the effects of time harmonics can be evaluated; however, it is difficult to assess the influence of space harmonics. Therefore, the radial pressure P_r was calculated using the Maxwell stress tensor equation through the air-gap flux density in time and space. The Maxwell stress tensor equation is as follows (1). In (1), μ_0 is the magnetic permeability of free space, B_{gr} is the air gap flux density of radial component, and B_{gt} is the air gap flux density of tangential component. Since B_{gt} has a relatively low value compared to B_{gr}, it can be considered negligible, and the equation can be rearranged as follows.

$$P_r(\alpha, t) = \frac{1}{2\mu_0}\left(B_{gr}^2 - B_{gt}^2\right) \approx \frac{1}{2\mu_0}B_{gr}^2 \quad (1)$$

The air gap flux density derived through two-dimensional (2-D) finite elements analysis (FEA) and P_r derived through (1) were expressed as a spectrum through Fourier series expansion. The waveform and spectra of the B_{gr} according to space and time changes of the 6-pole, 9-slot model are shown in Fig. 3 (a) and (b), and the waveform and spectra of P_r are as shown in Fig. 3 (c) and (d). Since the deformation of a cylindrical structure while neglecting the tooth and slot geometry, is inversely proportional to the fourth power of the order [3], it is necessary to design the motor to increase the lowest order component of P_r. Finally, the 2-D FEA results under PWM current excitation were mapped onto the 3-D mechanical frequency analysis.

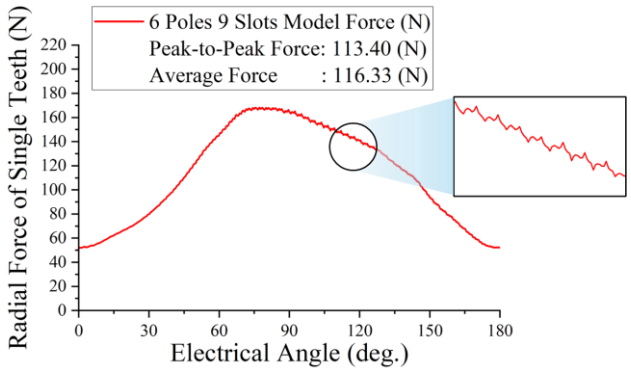


Fig. 2. Excitation force graph reflecting PWM current.

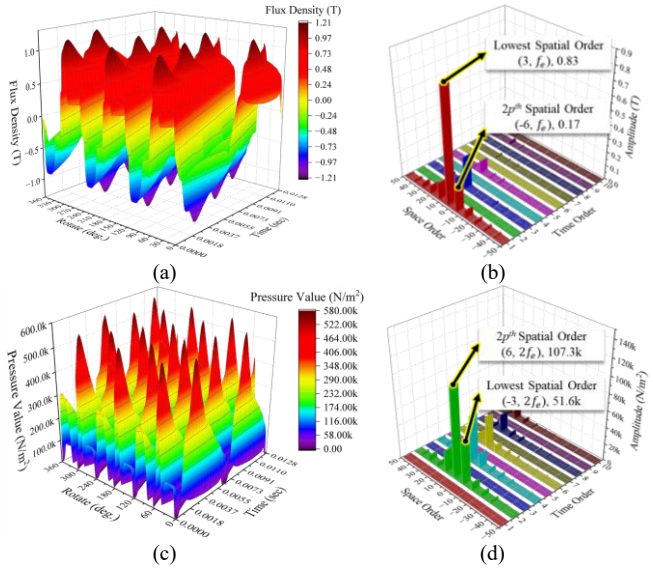


Fig. 3. Waveforms and spectrum of air-gap flux density and pressure for 6-pole, 9-slot model. (a) waveform of flux density. (b) spectrum of flux density. (c) waveform of air-gap pressure. (d) spectrum of pressure.

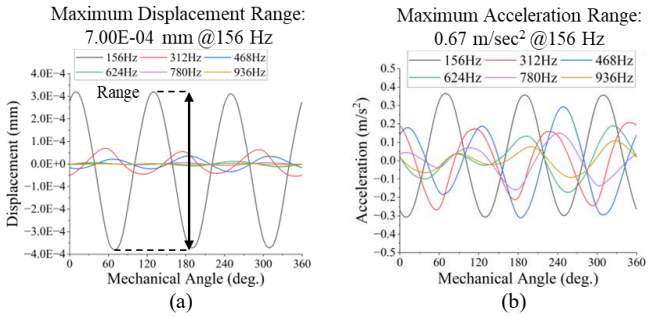


Fig. 4. Displacement and acceleration of the stator outer side of the 6-pole, 9-slot model. (a) displacement waveform. (b) acceleration waveform.

The displacement response at the stator outer surface as a function of input frequency is shown in Fig. 4(a), and the acceleration response is shown in Fig. 4(b). Since the lowest space order in Fig. 3 (d) is 3, can confirm that the period of the waveform in Fig. 4 (a) and (b) is 3. In the subsequent full paper, the electrical and vibration characteristics of each model, including manufacturing cost, will be derived and comparatively analyzed.

Acknowledgemt

This study is supported by research funds from the Ministry of Trade, Industry and Energy and the Korea Evaluation Institute of Industrial Technology (Project No. RS-2024-00431941).

References

[1] I. Petrov, P. Lindh, M. Niemelä, E. Scherman, and J. Pyrhönen, "High torque-density IPMSM rotor pole geometry adjustment for smooth torque," *IEEE Access*, vol. 7, pp. 52650–52658, 2019.

[2] S. Chen, C. -Y. Hsiao, L. Yao, F. Yu, Y. Wang and J. -X. Shen, "Comparative Analysis of Magnet Demagnetization in FSCW and ISDW IPM Machines with Various Rotor Topologies," *2020 23rd International Conference on Electrical Machines and Systems (ICEMS)*, Hamamatsu, Japan, 2020, pp. 201-205

[3] Y. Mao, W. Zhao, S. Zhu, Q. Chen and J. Ji, "Vibration Investigation of Spoke-Type PM Machine With Asymmetric Rotor Considering Modulation Effect of Stator Teeth," *IEEE Trans. on Ind. Electron.*, vol. 68, no. 10, pp. 9092-9103, Oct. 2021.